Experimental Validation of a Fault-Tolerant Hexacopter with Tilted Rotors

Juan I. Giribet[1,2], Claudio D. Pose[1], Alejandro S. Ghersin[3,2], and Ignacio Mas[2,4]
[1] Grupo de Procesamiento de Señales, Identificación y Control (GPSIC), Departamento de Ingeniería Electrónica, Facultad de Ingeniería Universidad de Buenos Aires (FIUBA), Argentina.
[2] Consejo Nacional de Investigaciones Científicas y Técnicas (CONICET), Argentina.
[3] Departamento de Ingeniería Electrónica, Instituto Tecnológico de Buenos Aires (ITBA), Argentina.
[4] Centro de Sistemas y Control (CeSyC), Departamento de Matemática, ITBA.
Email: jgiribet@conicet.gov.ar; cldpose@fi.uba.ar; aghersin@itba.edu.ar; imas@itba.edu.ar

***Abstract*—Recently, research reporting the advantages of flying with tilted-motor multicopters has surfaced. Particularly, it has been theoretically proven that in the case of a complete failure of one of the motors in a hexagon-shaped hexacopter, complete altitude and attitude control can be maintained. In this work, these theoretical results were experimentally validated.**

***Index Terms*—Fault tolerance, multirotor vehicles, unmanned aerial vehicles**

I. Introduction

Recent advances in mobile robotics have boosted the research and development of unmanned aerial vehicles (UAVs). At a steady pace, ground piloted semi-autonomous as well as completely autonomous UAVs are beginning to replace manned systems in different applications, where repetitive and/or dangerous tasks are carried out.

Over the last few years, micro UAVs (mUAVs), in particular those with a multirotor configuration, have gained great popularity due to their availability and moderate cost. Little or no experience is needed to fly them and a person with little knowledge of the risks involved is completely capable of operating a mUAV.

As it is widely known, it is possible to carry out attitude and altitude control maneuvers with a multirotor through independently commanding the speed of the vehicle's motors. Multirotors present several advantages for a wide range of users and applications, taking advantage of their ability to vertically take-off and hold their position in the air. Recently, research reporting the advantages of flying with tilted-motor multicopters has surfaced [1]-[3]. Within these advantages, a study of fault tolerance for the hexagon-shaped hexarotor can be found in [3]. Previous work addressing the fault-tolerant control of mUAVs can be found in several references [4]-[9].

As a follow up of the research presented in [3], this work presents the experimental results considering the complete failure of one motor in a hexagon-shaped hexa-rotor. As it was theoretically proven (see [3]), a hexagon-shaped hexacopter, in which the axes of rotation of all motors are symmetrically tilted toward the vehicle's vertical axis, should be capable of keeping full altitude and attitude control in the case of complete failure in one of its motors. The fact that with this usual set-up, i.e., with the axes of rotation of all motors being parallel to the vehicle's vertical axis, fault tolerance cannot be achieved [4], which was also proven in [3].

It is worth mentioning that the results of [3] were also validated through simulations in [10], [11]. On the other hand, successful results were reported in [12] regarding experimental flights carried out with partial failure in one of the motors. The purpose of this work is to experimentally prove the theoretical results reported in [3].

II. Multirotor Vehicle Model

As in [3], it is assumed that the spinning direction of each motor cannot be inverted. As a consequence, each motor/propeller set in a multirotor is capable of exerting a force $f_i \geq 0$ on the direction of its spinning axis and a torque m_i on the same axis. The flight computer controls each motor's speed through a pulse width modulated (PWM) signal $u_i \in [0, 100\%]$. It is assumed that $f_i = k_f u_i$ and $m_i = (-1)^i k_t u_i$ where k_f and k_t are constants that depend on the characteristics of the motor/propeller set. The alternating sign of m_i is due to the motors' spinning directions, which in these vehicles is alternated for consecutive motors (see Fig. 1).

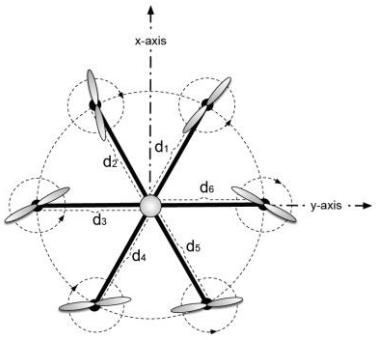

Figure 1. The rotor disposition of a hexacopter (top-view).

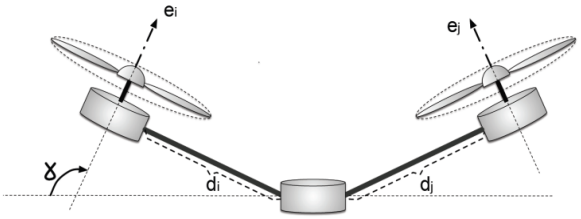

Figure 2. The rotor disposition of a hexacopter (side-view)

Fig. 1 and Fig. 2 show the proposed structure and rotor disposition for the fault-tolerant vehicle. The total vertical thrust F_z on the vehicle's z axis will be positive. If the maximum possible vertical thrust is desired, then the γ angle should be selected as $\gamma = 90°$. This is the standard configuration for this kind of vehicle, but such a situation does not allow for fault tolerance.

For the sake of clarity, the α parameter will be introduced:

$$\alpha = \alpha(\gamma) = \frac{k_t\, cos(\gamma)}{k_f \sqrt{3}\, l\, sin(\gamma)} \tag{1}$$

where $l = |d_i|$ is the distance from the center of mass of the vehicle to the rotor (arm length). It is assumed that $\gamma \in (0°, 180°)$. Note that in the standard configuration (i.e., $\gamma = 90°$) $\alpha = 0$.

In order to have full attitude control, the vehicle's actuators should be able to exert a torque $M = (M_x, M_y, M_z) \in \mathbb{R}^3$ in any arbitrary direction when commanded with the magnitude constraints given by the motors' saturation (i.e., 0% or 100% PWM).

The relationship between the force produced by the rotor set $f_i \geq 0$ with the torque and the vertical thrust (M_x, M_y, M_z, F_z) is given by the following equation:

$$\begin{bmatrix} M_x \\ M_y \\ M_z \\ F_z \end{bmatrix} = A(\gamma, \alpha) \cdot f, f = \begin{bmatrix} f_1 \\ \vdots \\ f_6 \end{bmatrix} \tag{2}$$

where the matrix $A = A(\gamma, \alpha) \in \mathbb{R}^{4\times 6}$ is

$$\begin{matrix} \frac{k_t}{k_f}c(\gamma) \\ \frac{k_t}{k_f}c(\gamma) \\ \frac{k_t}{k_f}s(\gamma) \\ s(\gamma) \end{matrix} \begin{bmatrix} -1 & \frac{\alpha+1}{2\alpha} & \frac{\alpha+1}{2\alpha} & -1 & \frac{\alpha-1}{2\alpha} & \frac{\alpha-1}{2\alpha} \\ -\frac{1}{\sqrt{3}\alpha} & \frac{3\alpha-1}{2\sqrt{3}\alpha} & -\frac{3\alpha-1}{2\sqrt{3}\alpha} & \frac{1}{\sqrt{3}\alpha} & \frac{3\alpha+1}{2\sqrt{3}\alpha} & -\frac{3\alpha+1}{2\sqrt{3}\alpha} \\ 1 & -1 & 1 & -1 & 1 & -1 \\ 1 & 1 & 1 & 1 & 1 & 1 \end{bmatrix}$$

where $s(\gamma), c(\gamma)$ represent $\sin(\gamma)$ and $\cos(\gamma)$, respectively. It is important to remark that, as

$$\frac{k_t \cos(\gamma)}{\alpha} = kf\sqrt{3}l\sin(\gamma)$$

Matrix $A(\gamma, \alpha)$ is a well-defined matrix for every value of α.

The problem of finding a force set $f_i \geq 0$ to achieve a torque of $M \in \mathbb{R}^3$ and a vertical force of $F_z > 0$ is solved by finding the solutions to Equation (2). Usually this problem is solved using the Moore-Penrose pseudoinverse (MP-PSI) of A, denoted as $A^\dagger$, and the solution is as follows:

$$\begin{bmatrix} f_1 \\ \vdots \\ f_6 \end{bmatrix} = A(\gamma, \alpha)^\dagger \cdot \begin{bmatrix} M_x \\ M_y \\ M_z \\ F_z \end{bmatrix} + w \tag{3}$$

where $w \in N(A)$ is a vector that belongs to the null space of $A = A(\gamma, \alpha)$. Most often, $w = 0$ is picked, because the minimum norm solution of Equation (2) is obtained, meaning the minimum energy f is used. Nevertheless, it is important to consider that additional conditions are needed to guarantee that this solution satisfies $f_i \geq 0$ for $i = 1, \ldots, 6$ (see [3, 11]).

A. Motor failure and fault tolerance analysis

It will be assumed that the motor failure is total, which means that if a rotor fails, it is incapable of generating any thrust or torque at all. For instance, if rotor 2 fails then $f_2 = 0$. Consequently, if a torque of $M = (M_x, M_y, M_z) \in \mathbb{R}^3$ and a vertical force of $F_z > 0$ are desired, it should be analyzed if there exists any solution of Equation (2) with $f_2 = 0$.

One way to model the failure is by redefining the A matrix. Given a failure in motor "*i*", the new matrix denoted $A_i \in \mathbb{R}^{4x6}$, is defined by replacing the *i*-th column of "*A*" with zeros. Then, for a failure in rotor 2, the matrix A_2 is defined as

$$\begin{matrix} \frac{k_t}{k_f}c(\gamma) \\ \frac{k_t}{k_f}c(\gamma) \\ \frac{k_t}{k_f}s(\gamma) \\ s(\gamma) \end{matrix} \begin{bmatrix} -1 & 0 & \frac{\alpha+1}{2\alpha} & -1 & \frac{\alpha-1}{2\alpha} & \frac{\alpha-1}{2\alpha} \\ -\frac{1}{\sqrt{3}\alpha} & 0 & -\frac{3\alpha-1}{2\sqrt{3}\alpha} & \frac{1}{\sqrt{3}\alpha} & \frac{3\alpha+1}{2\sqrt{3}\alpha} & -\frac{3\alpha+1}{2\sqrt{3}\alpha} \\ 1 & 0 & 1 & -1 & 1 & -1 \\ 1 & 0 & 1 & 1 & 1 & 1 \end{bmatrix}$$

Consequently, the force-torque equation when rotor 2 fails is given by:

$$\begin{bmatrix} f_1 \\ \vdots \\ f_6 \end{bmatrix} = A_2(\gamma, \alpha)^\dagger \cdot \begin{bmatrix} M_x \\ M_y \\ M_z \\ F_z \end{bmatrix} + \beta \begin{pmatrix} \frac{3}{4}(\alpha-1)\left(\alpha+\frac{1}{3}\right) \\ 0 \\ -\frac{3}{4}(\alpha+1)\left(\alpha-\frac{1}{3}\right) \\ -\frac{3}{4}\left(\alpha^2+\frac{1}{3}\right) \\ \alpha \\ \frac{3}{4}\left(\alpha^2+\frac{1}{3}\right) \end{pmatrix} \tag{4}$$

where $A_2^\dagger$ is given by Equation (5) and

$$w = \begin{pmatrix} \frac{3}{4}(\alpha-1)\left(\alpha+\frac{1}{3}\right) \\ 0 \\ -\frac{3}{4}(\alpha+1)\left(\alpha-\frac{1}{3}\right) \\ -\frac{3}{4}\left(\alpha^2+\frac{1}{3}\right) \\ \alpha \\ \frac{3}{4}\left(\alpha^2+\frac{1}{3}\right) \end{pmatrix}$$

is a vector that belongs to the null space of A_2 and satisfies the restriction $w_2 = 0$. Furthermore, all the vectors in $N(A_2)$ satisfying this restriction are written as βw with $\beta \in \mathbb{R}$ parametrizing the set of all solutions for Equation (4) with the restriction $f_2 = 0$.

$$A_2(\gamma,\alpha)^{\dagger} = \begin{pmatrix} -\frac{\alpha(15\alpha^3+9\alpha^2+9\alpha-1)\sec(\gamma)}{4k_t(3\alpha^2+1)^2} & -\frac{\alpha(9\alpha^3+27\alpha^2-9\alpha+5)\sec(\gamma)}{4\sqrt{3}k_t(3\alpha^2+1)^2} & \frac{(3\alpha+1)^2\csc(\gamma)}{12k_t(3\alpha^2+1)} & \frac{(\alpha-1)^2\csc(\gamma)}{12\alpha^2+4} \\ 0 & 0 & 0 & 0 \\ \frac{3\alpha(\alpha+1)^3\sec(\gamma)}{4k_t(3\alpha^2+1)^2} & -\frac{\alpha(3\alpha-1)^3\sec(\gamma)}{4\sqrt{3}k_t(3\alpha^2+1)^2} & \frac{(1-3\alpha)^2\csc(\gamma)}{6k_t(6\alpha^2+2)} & \frac{(\alpha+1)^2\csc(\gamma)}{12\alpha^2+4} \\ -\frac{\alpha(3\alpha-1)\sec(\gamma)}{4(3k_t\alpha^2+k_t)^2} & \frac{\sqrt{3}\alpha(\alpha+1)\sec(\gamma)}{4(3k_t\alpha^2+k_t)^2} & -\frac{\csc(\gamma)}{4k_t} & \frac{\csc(\gamma)}{4} \\ \frac{\alpha(3\alpha^3-1)^2\sec(\gamma)}{k_t(3\alpha^2+1)^2} & \frac{\alpha(9\alpha^3+1)^2\sec(\gamma)}{\sqrt{3}k_t(3\alpha^2+1)^2} & \frac{\csc(\gamma)}{3k_t(3\alpha^2+1)} & \frac{\alpha^2\csc(\gamma)}{3\alpha^2+1} \\ \frac{\alpha(3\alpha-1)\sec(\gamma)}{4(3k_t\alpha^2+k_t)} & -\frac{\sqrt{3}\alpha(\alpha+1)\sec(\gamma)}{4(3k_t\alpha^2+k_t)} & -\frac{\csc(\gamma)}{4k_t} & \frac{\csc(\gamma)}{4} \end{pmatrix} \quad (5)$$

To analyze why the standard design used for an hexacopter is not fault tolerant but becomes so when the motors are tilted, it suffices to analyze the last column of matrix $A_2^{\dagger}$. It is easy to see that its components are strictly positive given that $\alpha \neq 0$ and $|\alpha| \neq 1$. Hence, it is always possible to achieve a torque in any direction. In fact, if a torque $M = (M_x, M_y, M_z)$ is to be exerted, it suffices to choose $F_z > 0$, which is large enough to obtain $f_i \geq 0$ (note that from Equation (4), f_2 corresponding to a failing rotor is always $f_2 = 0$). Nevertheless, if $\alpha = 0$ or $|\alpha| = 1$, this is not possible. For instance, if $\alpha = 0$, that is, if the rotors are not tilted, the force exerted by motor 5 (opposite to failing motor 2) is given by

$$f_5 = \left(\frac{\alpha(3\alpha^3-1)\sec(\gamma)}{k_t(3\alpha^2+1)^2}\right)M_x + \\ + \left(\frac{\alpha(9\alpha^3+1)\sec(\gamma)}{\sqrt{3}k_t(3\alpha^2+1)^2}\right)M_y + \left(\frac{\csc(\gamma)}{9k_t\alpha^2+3k_t}\right)M_z$$

which does not depend on F_z or β. So, there exists a torque $M = (M_x, M_y, M_z)$ that does not allow for positive solutions with $f_i \geq 0$ for Equation (4). If $\alpha = 0$, the vehicle is incapable of exerting the torque

$$M = -\epsilon\left(\frac{\alpha(3\alpha^3-1)\sec(\gamma)}{k_t(3\alpha^2+1)^2}, \frac{\alpha(9\alpha^3+1)\sec(\gamma)}{\sqrt{3}k_t(3\alpha^3+1)^2}, \frac{\csc(\gamma)}{9k_t\alpha^2+3k_t}\right)$$

for any value of $\epsilon > 0$, if commanded.

The same happens if $|\alpha| = 1$. This means that if the rotors are placed with $\gamma = 90°$ or in a way such that $|\tan(\gamma)| = \frac{k_t}{k_f\sqrt{3}l}$, the vehicle will not be able to exert torques in a certain direction, losing its degrees of freedom. On the other hand, for any other value of γ, it is possible to achieve any maneuver thus obtaining a 4DOF vehicle. The next issue to be solved is how to choose γ.

III. Proposed Design for a Fault-Tolerant Hexacopter

Evidently, to maximize vertical thrust, the optimal disposition is that with $\gamma = 90°$, that is, $\alpha = 0$. At the same time, to achieve fault tolerance it is needed that $\alpha \neq 0$.

Depending on the selected value of γ and given a bound for the torque exerted, there exists one particular direction in which that torque is most difficult to achieve (the one that stresses the motors the most), which is called the worst-case torque (w.c.t.). Fig. 3 shows, for a vehicle with a given set of constants k_f, k_t, l, the necessary vertical thrust F_z needed to achieve the w.c.t. for different values of $\theta = 180° - \gamma$.

In this figure, it can be seen that when $\gamma = 90°$ or when $|\tan(\gamma)| = \frac{k_t}{k_f\sqrt{3}l}$ (corresponding to γ values of approximately 45° and 135°), $F_z \to \infty$, as there is a direction in which the torque cannot be exerted. On the other hand, if $\gamma = 73°$ or $\gamma = 107°$, the necessary vertical thrust is minimized. Additionally, it can be noted that for the latter values, slightly less than 5% vertical thrust is lost. Given that this loss is not considered significant, it would be a reasonable choice for the tilting angle.

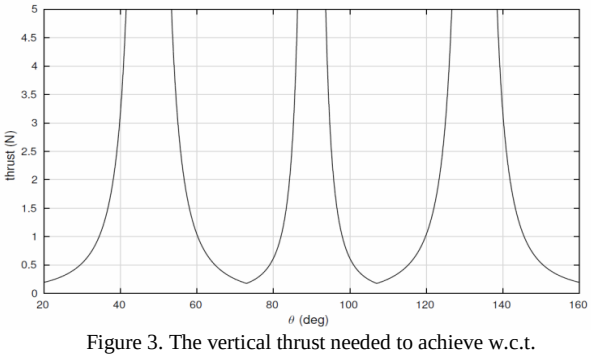

Figure 3. The vertical thrust needed to achieve w.c.t.

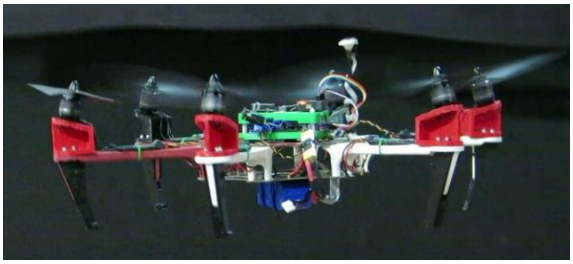

Figure 4. Hexarotor w/tilted motors with one in total failure.

Fig. 4 shows a picture of the hexacopter used in the experiments, flying with a total failure in one of its rotors. This vehicle is a commercial DJI F550 model modified for this work at the "Grupo de Procesamiento de Señales, Identificación y Control" Lab (Group for Signal Processing, Identification and Control - GPSIC) at the School of Engineering of the University of Buenos Aires. The flight computer as well as the navigation and control algorithms was also developed at the GPSIC.

From the point of view of fault tolerance, choosing $\gamma = 73°$ or $\gamma = 107°$ is the same due to symmetry. Nevertheless, there are other factors that make it preferable to choose $\gamma = 107°$. Firstly, it can be shown that in the case where the vehicle's arms are tilted upwards–rather than tilting just the motors–the vehicle's center of mass is lowered hence rendering a vehicle easier to stabilize. Secondly, tilting the arms upwards allows for a better field of view in the case when camera-type payloads are attached to the vehicle, which is not uncommon.

IV. Simulation Results

In the previous sections it was studied how it is possible to design a vehicle capable of maintaining full attitude and altitude control even when a failure occurs in one of its rotors. Although after the failure occurs the vehicle can exert torque in any direction, the magnitude of the achievable torque is lower when compared to the case when the vehicle flies with no motors failing. The size reduction in the set of reachable torques has an impact on the design of the control algorithm. The purpose of this section is to study this problem, which will establish a criterion for designing the vehicle's attitude control algorithm.

In a nominal situation, with the vehicle flying without failures, the control algorithm is designed in such a way that the vehicle can reach the desired torque values while keeping the operating point of the actuators in a suitable range. In this way, it is possible to fly with an agile vehicle, which is capable of rejecting any disturbances that may arise without deviating significantly from the desired trajectory.

When a failure occurs, if the control law remains the same, the remaining motors will be stressed, in order to achieve the same torque values. Furthermore, certain torque values will not be achieved if the motors saturate, which can be catastrophic from the point of view of the stability of the vehicle. To overcome this problem, it is necessary to modify the control law in such a way that the control torque values are attenuated. Therefore, when flying with five motors, the bandwidth of the control loop must be lowered, resulting in a vehicle with a slower response, guaranteeing that the actuators will not saturate.

Coupled with the actuator allocation model presented in Section II (see Eq. (2)), a 6DOF model was employed in the simulations carried out during this study (see the 6DOF ECEF quaternion based model in [13]). A first order low-pass filter was also included in the model, which accounts for motors' response to commands. Based upon a small roll and pitch angles hypothesis, assuming a diagonal inertia tensor for the vehicle with low angular rates, the simplified transfer functions for the roll (Φ), pitch (Θ) and yaw (Ψ) loops are as follows:

$$\frac{\Phi(s)}{M_X(s)} = \frac{1}{J_X\left(\frac{s}{p}+1\right)s^2},$$

$$\frac{\Theta(s)}{M_Y(s)} = \frac{1}{J_Y\left(\frac{s}{p}+1\right)s^2},$$

$$\frac{\Psi(s)}{M_z(s)} = \frac{1}{J_Z\left(\frac{s}{p}+1\right)s^2},$$

where M_X, M_Y and M_z are the corresponding torque values achieved by the actuator allocation algorithm. The "p" pole accounts for actuator low-pass dynamics.

PID control was applied by employing a loop–at–a–time strategy to control each of the vehicle's orientation angles. System identification was carried out based upon the closed loop data obtained without rotor failure in order to estimate all the model parameters. Assuming $J_X = J_Y$, the fitted values were:

$$J_{X,Y} = 0.0476 \text{ kg.m}^2$$

$$J_Z = 0.1094 \text{ kg.m}^2$$

$$p = 20.06 \frac{\text{rad}}{\text{sec.}}$$

The fitting of the identified system can be seen in Fig. 5. A grey-box approach was adopted to preserve the physical meaning of the model parameters (see [14], [15] for a discussion on this topic).

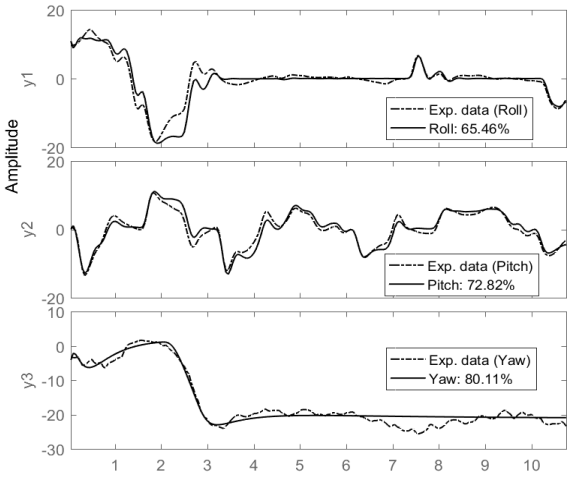

Figure 5. The fitted roll, pitch and yaw transfer functions

The approach followed for the design and tuning of the controllers is an issue that has been addressed in several publications (see [16]-[20]). The gains of the PID controllers were tuned based upon simulated and experimental results shown below:

Gains	K_d	K_p	K_i
Aggressive	0.9	5	6
Mild	0.9	1.4	1
Yaw	0.6	0.8	0.2

Tuning was carried out considering the transient response only. The "aggressive" gains set was employed for the identification experiments in the roll and pitch loops. The "mild" gains set was employed for the flight test under motor failure. The yaw gains set was used for yaw control throughout all experiments and simulations.

In regard the results of the simulations shown in Fig. 6, the simulated transient responses can be seen for the pitch axis. The curves are the result of a 1 Nm pulse disturbance torque on the pitch axis, from 5 to 15 s.

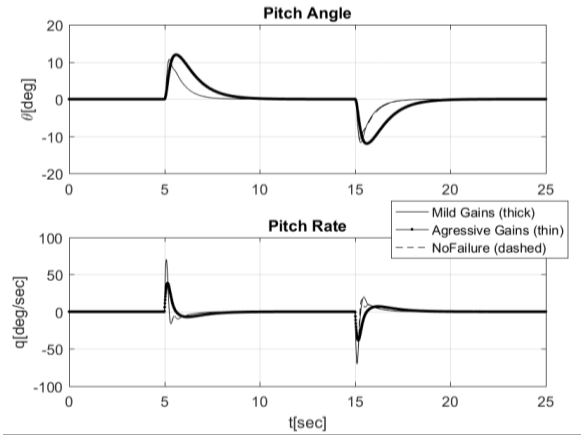

Figure 6. The response to the pulse dist. torque

The thin solid line as well as the dashed line shows the transient responses with the aggressive gains. The dashed lines reflect the response without motor failure. Barely any difference can be observed with the solid thin line, which exhibits the response with the aggressive gains under failure in motor 2. The solid thick line shows the response with the mild gains, which is slower and less responsive.

In regard the PWM signals, a remarkable difference can be observed in the simulated actuator signals, as shown in Fig. 7. Again, the dashed lines show the response without failure in the simulations. The solid thick and thin lines reflect the simulation with failure in motor 2 for the aggressive gains (thin lines) and for the mild gains (thick lines). Notice that motor number 5, the exact opposite of the failing one, is forced to greatly reduce its thrust and as a result, it ends up operating closer to 0% PWM. Note that with the aggressive gains, motor 5 is commanded to go below 0% PWM, something that cannot be achieved. On the other hand, the mild gains avoid commanding the motor below 0% PWM in this particular case.

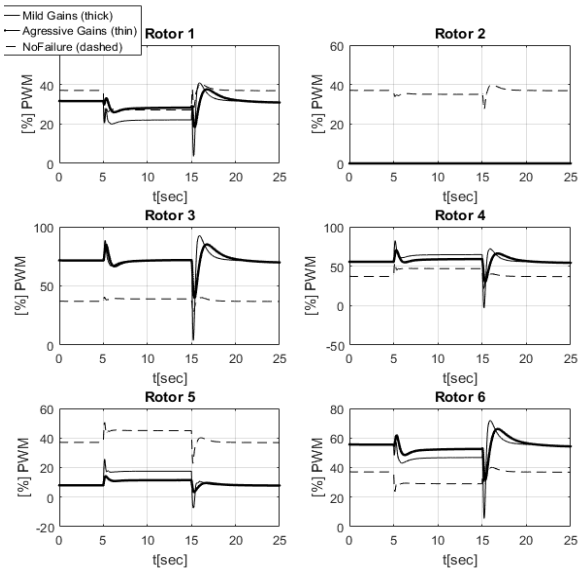

Figure 7. The simulated PWM signals.

As it will be further illustrated in the following section, in practice, driving any motor to a complete stop in flight is unacceptable and potentially catastrophic as the restarting of a brushless motor introduces heavy transient disturbances to the vehicle, potentially destabilizing it. Even though in the simulation the control system with aggressive gains correctly recovers from under-saturating motor 5, this cannot be applied in practice. Other not simulated phenomena, such as the ground effect, prevent the use of aggressive gains in practice under failure.

V. Experimental Results

The purpose of this section is to show the experimental results obtained in several hexacopter flights, with and without failure. The problem of fault detection is not addressed in this work, as the objective is to experimentally demonstrate that the vehicle can fly with a complete failure in one motor while keeping the ability to perform different maneuvers. The experiments were carried out using a DJI F550 model vehicle with 920KV motors with 9545 propellers and a 4s LiPo battery. A set of 3D printed supplements were employed in order to modify the original $\gamma = 90°$ mounting angle of the motors to a $\gamma = 107°$ modified mounting angle.

The experiment carried out involves taking off the ground with a shut-down motor, flying for approximately two minutes while performing different maneuvers and then landing safely [21]. The results corresponding to this flight are shown in several graphics due to the amount of data, to obtain a clearer understanding of the experiment. Also, there are two additional experiments to demonstrate the yaw maneuvering capabilities and performance.

Fig. 8 starts with the vehicle take-off and then several seconds of vehicle hovering, while adjusting the bias settings of the radio control, a procedure usually carried out in order to allow the vehicle to remain in a hovering state when no commands are sent over the radio control. Later, commands of an impulsive kind are given to the vehicle in the roll and pitch directions.

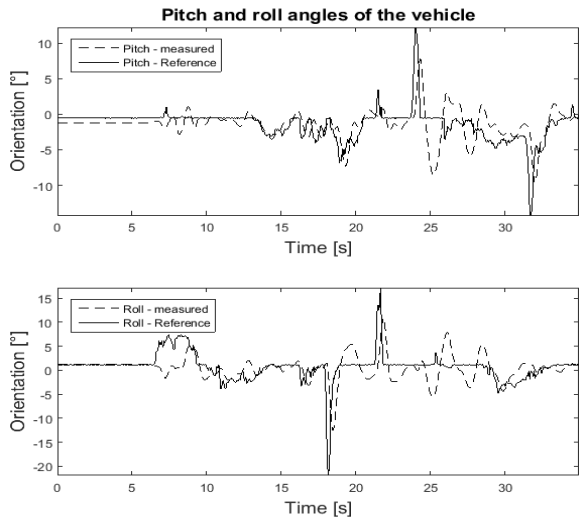

Figure 8. The pitch and roll angles during take-off

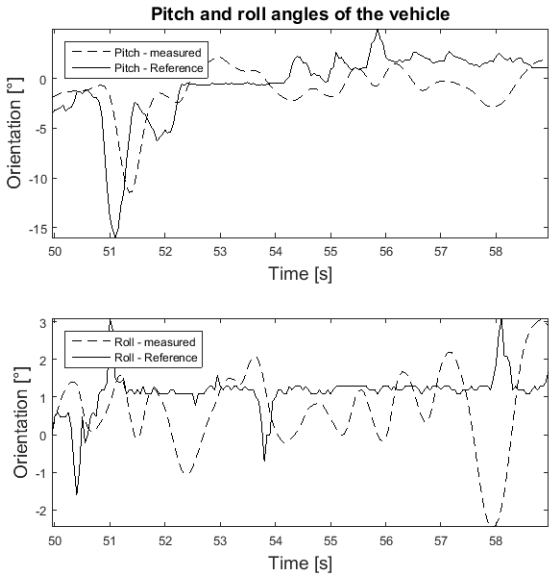

Figure 9. The pitch and roll angles during hovering.

In Fig. 9, the data corresponding to the middle of the flight are presented. Here a good response to a pitch command is shown, followed by several seconds of the vehicle in a hovering state. It is shown that during hovering, the pitch and roll angles remain around $\pm 2.5°$ of the reference, something that can be considered as an acceptable performance.

For the last part of the flight more maneuvers were executed independently in both axes, as well as in both axes at the same time, as shown in Fig. 10. Finally, the vehicle landed safely at 103 s.

The PWM signals commanded to each rotor for the full flight are presented in Fig. 11. Motor number 2 always has its PWM at zero, as it is the failing motor. Note that the PWM of motor 5, located opposite to the failing motor, is significantly lower than the rest, (due to symmetry, with motor 5 off, hovering is theoretically achievable as long as there are no perturbations). Also, it can be seen that motor 5 is limited to around 14% of the PWM. In real applications, the rotors start operating at some value between 10% and 15% of the PWM (depending on the motor) and lower values will turn it off. Because the motor start is non-linear (if the motor is off, when it is turned on it can start rotating in the wrong direction before going in the right one due to its construction) the off state of the motors was avoided by limiting the PWM value to 14%, where the motors turn at very low speed and produce very little thrust, but remain on.

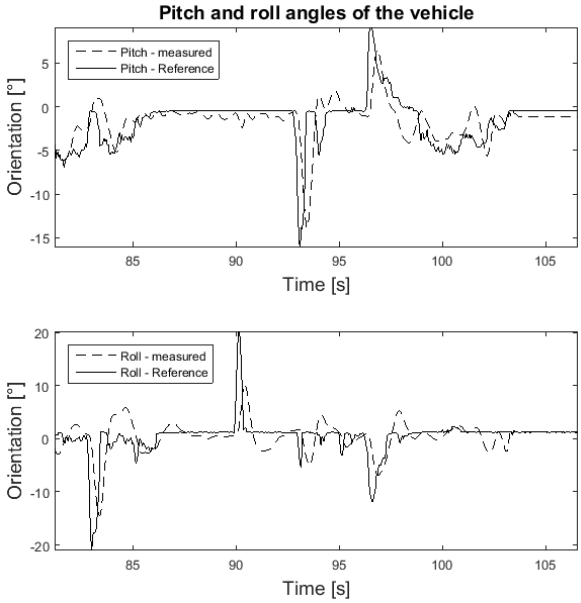

Figure 10. The pitch and roll angles during landing.

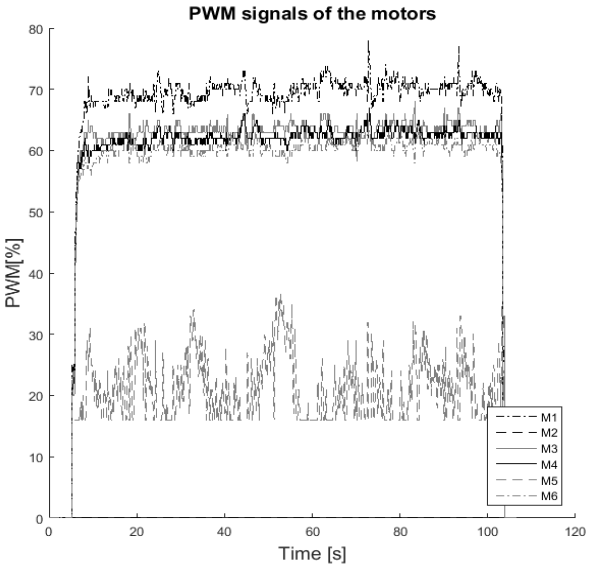

Figure 11. The PWM signals.

The rest of the motors are at similar PWM values with motors 1 and 3 being the most stressed because they are the ones next to the failing motor and have to provide compensating thrust.

The yaw maneuvering results are presented in Fig. 12 and 13 with each one representing a different direction of rotation. This is of interest because yaw maneuvers are the most affected when a motor failure takes place and, as the failing motor only exerts torque in the z axis in one direction, the torque achievable in that direction is lower, while the torque in the opposite direction presents no

problems. Fig. 12 shows a yaw maneuver carried out in the most relaxed direction. It can be seen that the reference is perfectly followed, and the system performs well. On the other hand, Fig. 13 presents a yaw maneuver carried out in the opposite direction, where the performance is poorer. Some oscillations can also be seen. It can be said that both experiments had nevertheless acceptable results.

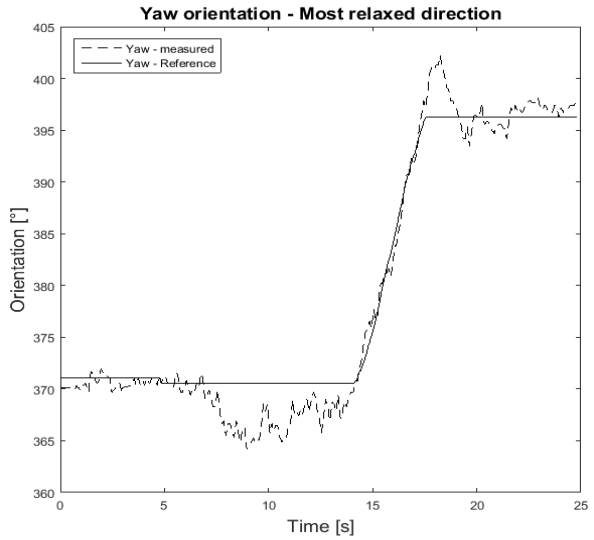

Figure 12. The yaw maneuver in the most relaxed direction.

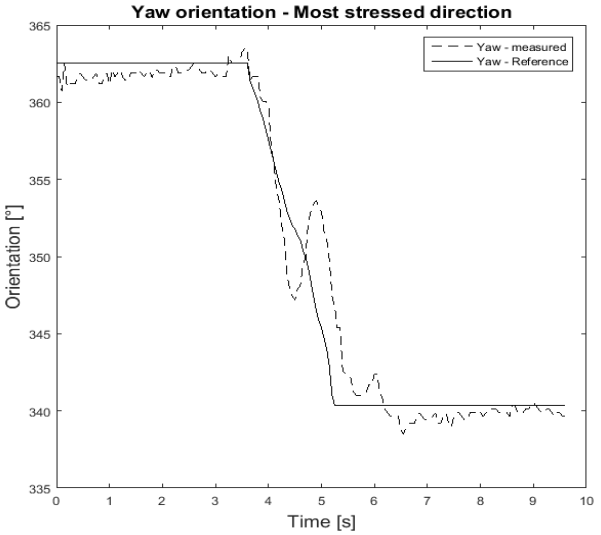

Figure 13. The yaw maneuver in the most stressed direction.

VI. Conclusions

This work provides conclusive experimental results backing up the theoretical and simulated results previously presented in the literature. As stated in the previous work, actuator allocation is a key aspect as far as fault tolerance is concerned in multirotors.

A key conclusion is concerned with the fact that the control gains have to be adjusted with respect to the nominal gains tuned for the case where there is no motor failure. Even though from a theoretical point of view, a readjustment of the gains should not be necessary because the 4DOF control can be held with the motors tilted; in practice a softened control is suggested in order to fly the vehicle, unless a different strategy is implemented in order to deal with the saturations.

Further investigations to be carried out should address the quantitative aspects such as the most convenient choice of k_f, k_t for a motor/propeller set, as well as other architectures of motor/propeller set tilts with respect to other axes of the vehicles, which could render further performance improvements.

Other research directions point toward studying the analysis and design of the control laws so they can handle the actuator saturation systematically. An important observation obtained as a result of the experiments, is concerned with the fact that saturation due to motor shut down turned out to be more troublesome in practice than saturation due to a motor at full speed, a condition which could be more rarely commanded by the control system.

Acknowledgment

This work has been supported by the Universidad Nacional de la Patagonia Austral (PI29/C066), Agencia Nacional de Promoción Científica y Tecnológica, FONCYT PICT 2014–2055 and FONCYT PICT 2016-2016 (Argentina). Claudio Pose would like to thank to the Peruilh Foundation and the University of Buenos Aires for their support. Alejandro Ghersin's work is supported by the Instituto Tecnológico de Buenos Aires (ITBA), through grant ITBACyT 28.

References

[1] S. Rajappa, M. Ryll, H. H. Bulthoff, and A. Franchi, "Modeling, control and design optimization for a fully-actuated hexarotor aerial vehicle with tilted propellers," in *Proc. IEEE Int. Conf. on Robotics and Automation (ICRA)*, Washington, 2015.

[2] M. Ryll, D. Bicego, and A. Franchi, "Modeling and control of FAST-Hex: A fully-actuated synchronized-tilting hexarotor," in *Proc. IEEE/RSJ International Conference on Intelligent Robots and Systems*, Daejeon, 2016.

[3] J. I. Giribet, R. S. Sánchez Peña, and A. S. Ghersin, "Analysis and design of a tilted rotor hexacopter for fault tolerance," *IEEE Trans. on Aerospace and Electronics Systems*, vol. 52, no. 4, pp. 1555–1567, 2016.

[4] M. Achtelik, K. Doth, D. Gurdan, and J. Stumpf, "Design of a multi rotor MAV with regard to efficiency, dynamics and redundancy," in *Proc. AIAA Guidance, Navigation, and Control Conference*, 2012.

[5] K. Valavanis and G. Vachtsevanos, *Handbook of Unmanned Aerial Vehicles*, Dordrecht: Springer Netherlands, 2015.

[6] M. Saied, B. Lussier, I. Fantoni, C. Francis, H. Shraim, and G. Sanahuja, "Fault diagnosis and fault-tolerant control strategy for rotor failure in an octorotor," in *Proc. IEEE International Conference on Robotics and Automation*, 2015.

[7] H. Alwi and C. Edwards, "Fault tolerant control of an octorotor using LPV based sliding mode control allocation," in *Proc. American Control Conference*, 2013.

[8] D. Rotondo, F. Nejjari y V. Puig, "Robust Quasi-LPV model reference FTC of a quadrotor UAV subject to actuator faults," *International Journal of Applied Mathematics and Computer Science*, vol. 25, no. 1, pp. 7–22, 2015.

[9] T. Schneider, "Fault-tolerant multirotor systems," Master's thesis, Swiss Federal Institute of Technology (ETH), Zurich, 2011.

[10] G. Michieletto, M. Ryll, and A. Franchi, "Control of statically hoverable multi-rotor aerial vehicles and application to rotor-failure robustness for hexarotors," in *Proc. IEEE International Conference on Robotics and Automation*, Singapore, 2017.

[11] C. Pose, J. I. Giribet, and A. Ghersin, "Hexacopter fault tolerant actuator allocation analysis for optimal thrust," in *Proc.*

International Conference on Unmanned Aircraft Systems (ICUAS), Miami, 2017.
[12] J. Giribet, C. Pose, and I. Mas, "Fault tolerant control of a hexacopter with a tilted-rotor configuration," in *Proc. XVII Reunión de Procesamiento de la Información y Control*, Mar del Plata, Argentina, 2017.
[13] Mathworks. Aerospace Blockset User's Guide. (2017). [Online]. Available: http://cn.mathworks.com/help/pdf_doc/aeroblks/aeroblks.pdf
[14] P. Panizza, F. Riccardi, and M. Lovera, "Black-box and grey-box identification of the attitude dynamics for a variable-pitch quadrotor," *IFAC-PapersOnLine*, vol. 48, no. 9, pp. 061–066, 2015.
[15] X. Chen and L. Wang, "Step response identification of a quadcopter UAV using frequency-sampling filters," *IFAC-PapersOnLine*, vol. 48, no. 25, pp. 122–127, 2015.
[16] P. Pounds, R. Mahony, and P. Corke, "Modelling and control of a large quadrotor robot," *Control Engineering Practice*, vol. 18, pp. 691–699, 2010.
[17] X. Yu, C. Tong, and H. Li, "Flight control of a quadrotor under model uncertainties," *International Journal of Micro Air Vehicles*, vol. 7, no. 1, 2015.
[18] S. Sawyer, "Gain-scheduled control of a quadcopter UAV," Waterloo, ON, Canada: Ms. of Mathematics thesis, University of Waterloo, 2015.
[19] T. Bresciani, "Modelling, identification and control of a quadrotor helicopter," Lund: MSc theses, Department of Automatic Control Lund University, 2008.
[20] J. Velasco, S. Garcia-Nieto, R. Simarro, and J. Sanchis, "Control strategies for unmanned aerial vehicles under parametric uncertainty and disturbances: A comparative study," *IFAC-PapersOnLine*, vol. 48, no. 9, pp. 001–006, 2015.
[21] C. Pose and J. Giribet. Tilted rotor hexacopter flying with failure (Video). GPSIC-FIUBA, 2017. [Online]. Available: https://youtu.be/a3-R2M5xWGA

Juan I. Giribet received his Electronic Engineer degree from the University of Buenos Aires, Argentina (2003) and Ph.D. from the University of Buenos Aires (2009). He worked in the Argentinean Space Agency (CONAE) and as a consultant in aerospace applications for private companies. In 2006, he was Professor at the Technological Institute of Buenos Aires and in 2009 at the National University of Quilmes. Currently he is Professor at the University of Buenos Aires and researcher at the Instituto Argentino de Matemática "Alberto Calderón" - CONICET. Prof. Giribet is a senior member of the IEEE. Since 2014, he is Director of the Master's Program in Mathematical Engineering at the University of Buenos Aires and Director of the GPISC Lab.

Claudio D. Pose received his Electronic Engineer degree from the University of Buenos Aires, Argentina (2014) and he is currently a Ph.D. student working on the design of fault-tolerant control and navigation systems for micro aerial robots at the same university. Since 2016, he is Assistant Professor in the Mathematics Department at the School of Engineering of the University of Buenos Aires.
Currently he is doing an internship at the University of Applied Sciences and Arts of Italian Switzerland in the Telecom, Telemetry and High Frequency laboratory. Claudio Pose was awarded a scholarship from the Peruilh Foundation.

Alejandro S. Ghersin received his Electronic Engineering degree from the University of Buenos Aires, Argentina (2000), and Ph.D. from the same university (2009). He was with the Argentinean Space Agency, CONAE (1999–2006). He worked at the Departamento de Ciencia y Tecnología of the Universidad Nacional de Quilmes (2007–2008), joining the Departamento de Ingeniería Electrónica at the Instituto Tecnológico de Buenos Aires as Full Professor in 2009. After finishing his doctoral studies, he was admitted to the Argentinean Consejo Nacional de Investigaciones Científicas y Tecnológicas–CONICET. At present his line of work is the field of control systems applied to mobile robots.

Ignacio Mas received his Engineering degree in Electronics from the Universidad de Buenos Aires, Buenos Aires, Argentina and Ph.D. degree in Mechanical Engineering from Santa Clara University, Santa Clara, CA, USA. He was a satellite systems engineer and spacecraft systems designer at the NASA Ames Research Center. Dr. Mas is currently an Adjunct Researcher at the Argentine National Scientific and Technical Research Council (CONICET) and a Professor at the University of Buenos Aires (UBA), Buenos Aires, Argentina. His research interests include multi-robot systems, coordinated navigation and robot formation control.